

High Luminosity pp and $\bar{p}p$ Colliding Beam Straight
Section Designs

D.E. Johnson

April 13, 1979

A multi-stage, matched, low-beta long-straight section for the Energy Doubler has been designed and is described below. In its simplest form, this straight section design essentially duplicates the current "standard" doubler lattice and can be used for fixed target operation. Through the re-powering of four quadrupoles on two circuits, a β^* of approximately ten meters can be produced for pp collisions. The addition of a third quadrupole circuit driving existing magnets can produce lower values of β^* . With the addition of four more quadrupoles inside the long-straight free space, betas of one to two meters are obtainable in a manner which does not so disrupt the lattice functions elsewhere as to make machine operation doubtful. Finally by separately powering another two quadrupoles in regular cells adjacent to the long-straight section, a dispersion free low- β section can be obtained. The details of these designs, including tune adjustment, chromaticity corrections, etc., are presented in the following sections.

Geometrical layouts of doubler long-straight sections are shown in Fig. 1. The top drawing is that of the present doubler lattice as designed by T.L. Collins in TM-874. This has all of the quadrupoles running in series with the dipoles and with each other. By replacing the two inner pair of quadrupoles with considerably longer, independently powered, three-shell quadrupoles, as shown in the second line in Fig. 1, a pp colliding insertion can be produced. This type of insertion has been described at various meetings by T. Collins, and the one shown differs only slightly from his in terms of element lengths. With the four outer

quadrupoles running normally and the inner ones set at rather weak values, the lattice functions across this insertion can essentially duplicate those of the "standard" straight sections. By leaving quads #1 and #12 connected in series, turning off quads #2 and #11, and re-powering the inner quads, a β^* of some 10 meters can be obtained. Quadrupole settings for these cases are listed in Table I, plots of the lattice functions are shown in Figs. 2 and 3, and various machine parameters are listed in Table II. By adding additional power supplies to the other two pair of quadrupoles, one can obtain lower values of β^* , although beta max starts to increase rapidly.

With the insertion of four more long, strong, and independently powered quadrupoles, one can produce β^* on the order of one meter. This is the Type II low- β shown in Fig. 1. Table I lists quadrupole settings for minimum beta values of 1 and 2 meters, and the lattice functions are plotted in Figs. 4 and 5. Machine parameters for these cases are again listed in Table II. A few arbitrary decisions have been made at this point and should be mentioned.

1. Quadrupoles #3 and #10 are turned off. These could be missing, but it seemed easier to leave them and add new ones. They are useful to return to normal, fixed-target operation, and, at least in the one meter case, are not long enough to serve as one of the inner quads.
2. The lengths of the strong quadrupoles may have to increase slightly depending on the maximum gradient obtainable. A maximum value of approximately 26.8 kG/m at 1 TeV has been used. Slight differences could be accommodated - perhaps down to around 25 kG/m, but certainly not as much as if one went to two-shell quadrupoles.

Most of the objections raised with the previous low- β designs have been overcome in these designs - namely the maximum values of beta and dispersion have been brought down to believable sizes, and the dispersion mismatch throughout the ring is also relatively small. Further investigations of these designs show them to be quite liveable. The tune corrections needed, from 30, 10" correcting quads per sector, is easily handled, and the chromaticity corrections are also rather simple. Table III lists the effect of momentum on various machine parameters for

the low- β cases. The one parameters which could present a problem, the change in the maximum value of the beta, is plotted in Fig. 6. While the percentage change in the maximum beta is rather large, the correction system is the simplest possible - two independent sextupole families. By going to a larger number of circuits, a much smaller variation could be obtained. It should be noted that the momentum aperture discussed herein is for perfect magnets. Putting in actual field distributions shrinks the available aperture considerably.

Finally, the question of non-zero dispersion at the collision point has been considered, and a solution to overcome this problem has been found. This has not yet been studied in depth, but rather is presented as an existence proof. It consists of separately powering fourteen quadrupoles - the twelve of Type II, plus the next two downstream of the straight section, that is those at stations 14 and 15. A plot of lattice functions for this case is shown in Fig. 7, and this is described in Tables I and II. There are several points to be noted:

1. This was done for a 2-meter β^* . An initial attempt to do it for 1 meter failed.
2. The quadrupole at station 15 is definitely needed. Perhaps the one at station 14 could be run normally.
3. Quadrupole #12 is running too hard for a two-shell quad.
4. The tunes have not been properly rematched to 19.4. Completely making the dispersion zero is an extremely difficult process, and may not be possible for other tunes.
5. The dispersion at the crossing point is shown as 8 cm. This can be made to be zero.

Table I

Quadrupole Settings

(Values in kG/m for 1 TeV)

	Case A	Case B	Case C	Case D	Case E
Quad #	"normal"	$\beta^* = 10 \text{ m}$	$\beta^* = 2 \text{ m}$	$\beta^* = 1 \text{ m}$	$\beta^* = 2 \text{ m},$ $\eta^* = 0$
1	-760.3206	-760.3206	-159.4277	195.9240	-326.7387
2	760.3206	0	-530.2842	-690.3435	181.1120
3	481.9685	931.4100	0	0	-302.2334
4	-561.0630	-1023.1598	696.6825	677.6592	908.8754
5	-	-	-1032.4382	-1056.4156	-1039.4206
6	-	-	885.3317	1040.3000	932.9205
7	-	-	-885.3317	-1040.3000	-466.9477
8	-	-	1032.4382	1056.4156	1038.6460
9	561.0630	1023.1598	-696.6825	-677.6592	-654.7409
10	-481.9685	-931.4100	0	0	-75.5129
11	-760.3206	0	530.2842	690.3435	346.6425
12	760.3206	760.3206	159.4277	-195.9240	812.9308
13	normal	normal	normal	normal	-634.0335
14					702.6145
Correct. Quads	0	± 85.1889	± 75.9866	± 89.7900	± 89.7900

Table II

Machine Parameters

	"standard" lattice	Case A	Case B	Case C	Case D	Case E
Free space(m)	53.194	51.974	51.974	15.991	15.991	15.991
β_x^* (m)	72.7	73.9	10.3	2.0	1.0	2.0
η^* (m)	2.24	2.26	0.21	0.40	0.48	-0.08
$\eta^{*'}(\text{mrad})$	18.1	18.2	-6.4	144	298	4.7
$\beta_{x\text{max}}(\text{m})$	243	243	247	378	851	240
$\beta_{y\text{max}}(\text{m})$	243	243	252	380	868	618
$\eta_{\text{max}}(\text{m})$	6.0	6.0	8.6	9.5	10.5	7.5
$\eta_{\text{min}}(\text{m})$	1.1	1.1	-0.5	-3.3	-5.2	-0.1
Q_x	19.395	19.393	19.394	19.393	19.400	19.632
Q_y	19.434	19.432	19.434	19.432	19.441	19.205
ξ_x	-22.5	-22.5	-23.2	-25.2	-29.1	-24.6
ΔQ needed	-	-	-0.317	-0.283	-0.334	-

Table IIIMachine Parameters vs. $\Delta p/p$

$$\beta^* = 2 \text{ m}, \quad B''\ell)_F = 429 \text{ kG/m}, \quad B''\ell)_D = -733 \text{ kG/m}$$

$\Delta p/p(\%)$	$\beta^*(\text{m})$	$\eta^*(\text{m})$	$\eta_{\max}(\text{m})$	Q_x	Q_y
-.375	1.76	0.36	9.3	19.394	19.434
-.25	1.84	0.37	9.4	.393	.433
-.125	1.92	0.39	9.5	.393	.433
0	2.01	0.40	9.5	.393	.432
.125	2.10	0.42	9.6	.393	.433
.25	2.20	0.43	9.7	.393	.433
.375	2.30	0.44	9.7	.394	.434

$$\beta^* = 1 \text{ m}, \quad B''\ell)_F = 492 \text{ kG/m}, \quad B''\ell)_D = -842 \text{ kG/m}$$

$\Delta p/p(\%)$	$\beta^*(\text{m})$	$\eta^*(\text{m})$	$\eta_{\max}(\text{m})$	Q_x	Q_y
-.375	.77	.40	10.5	19.405	19.449
-.25	.84	.43	10.4	.402	.444
-.125	.92	.46	10.2	.401	.442
0	1.01	.48	10.5	.400	.441
.125	1.11	.51	10.8	.401	.442
.25	1.24	.53	11.0	.402	.444
.375	1.38	.55	11.2	.405	.449

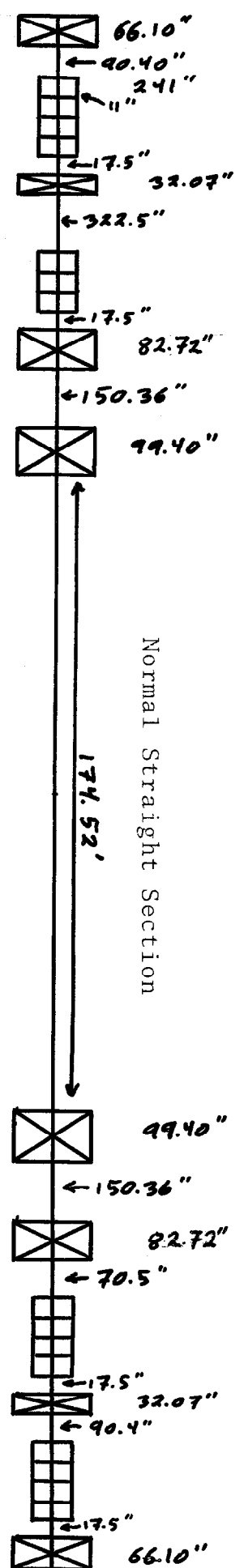
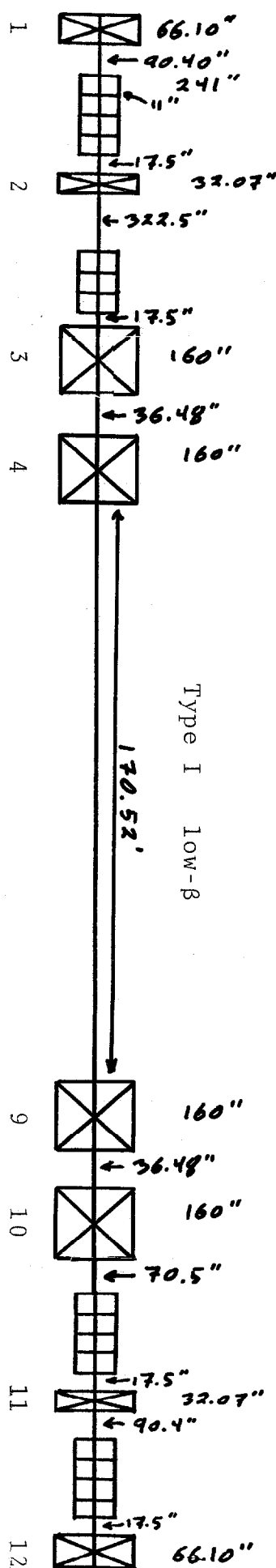
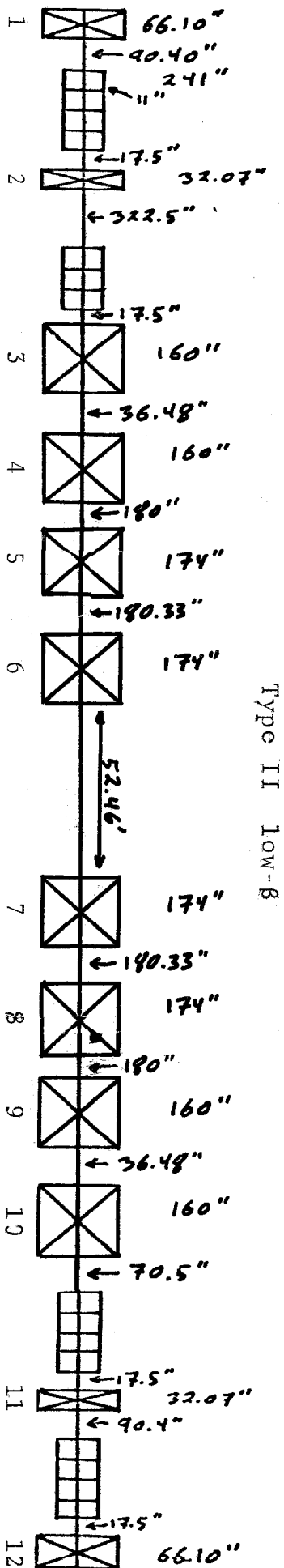
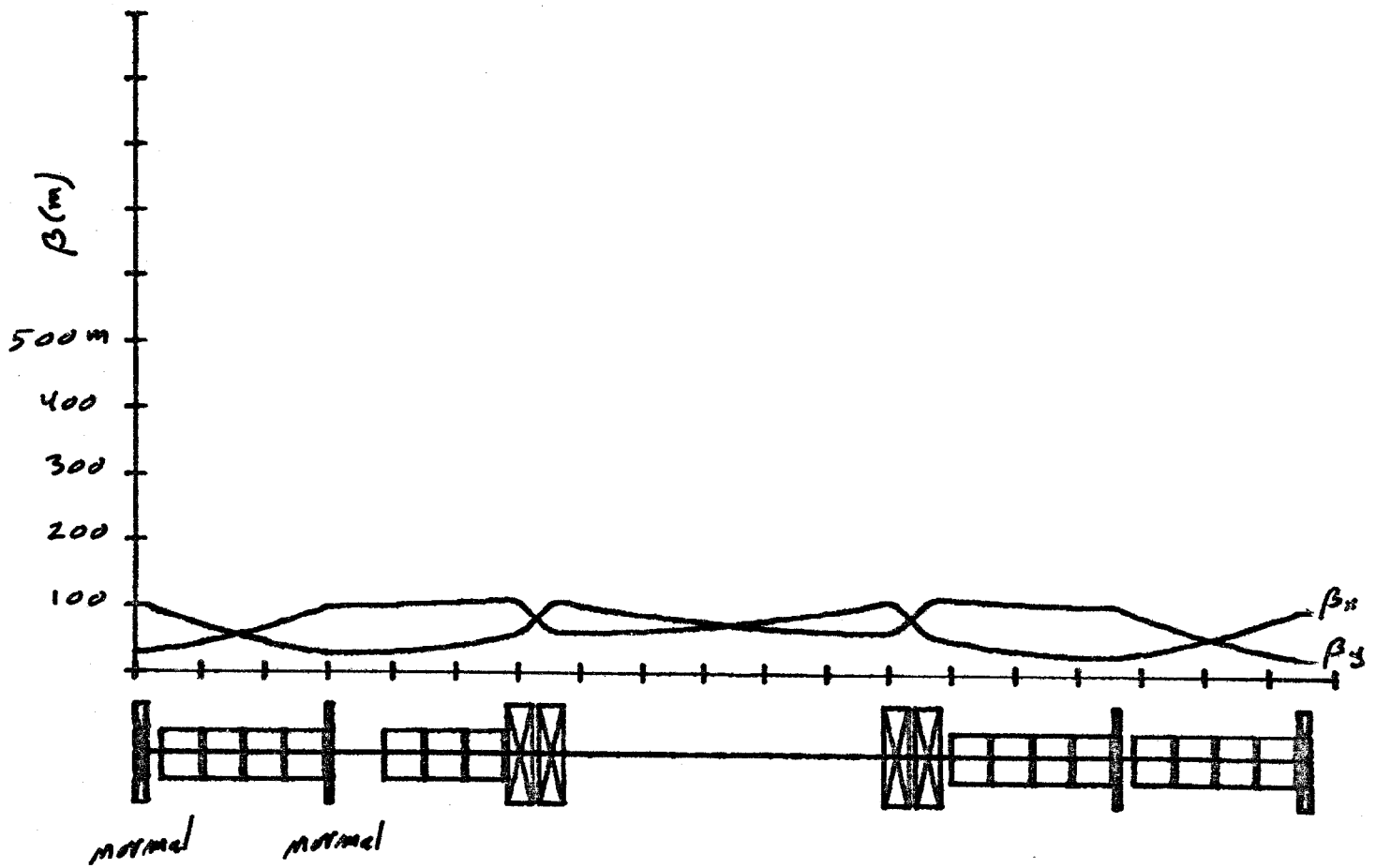


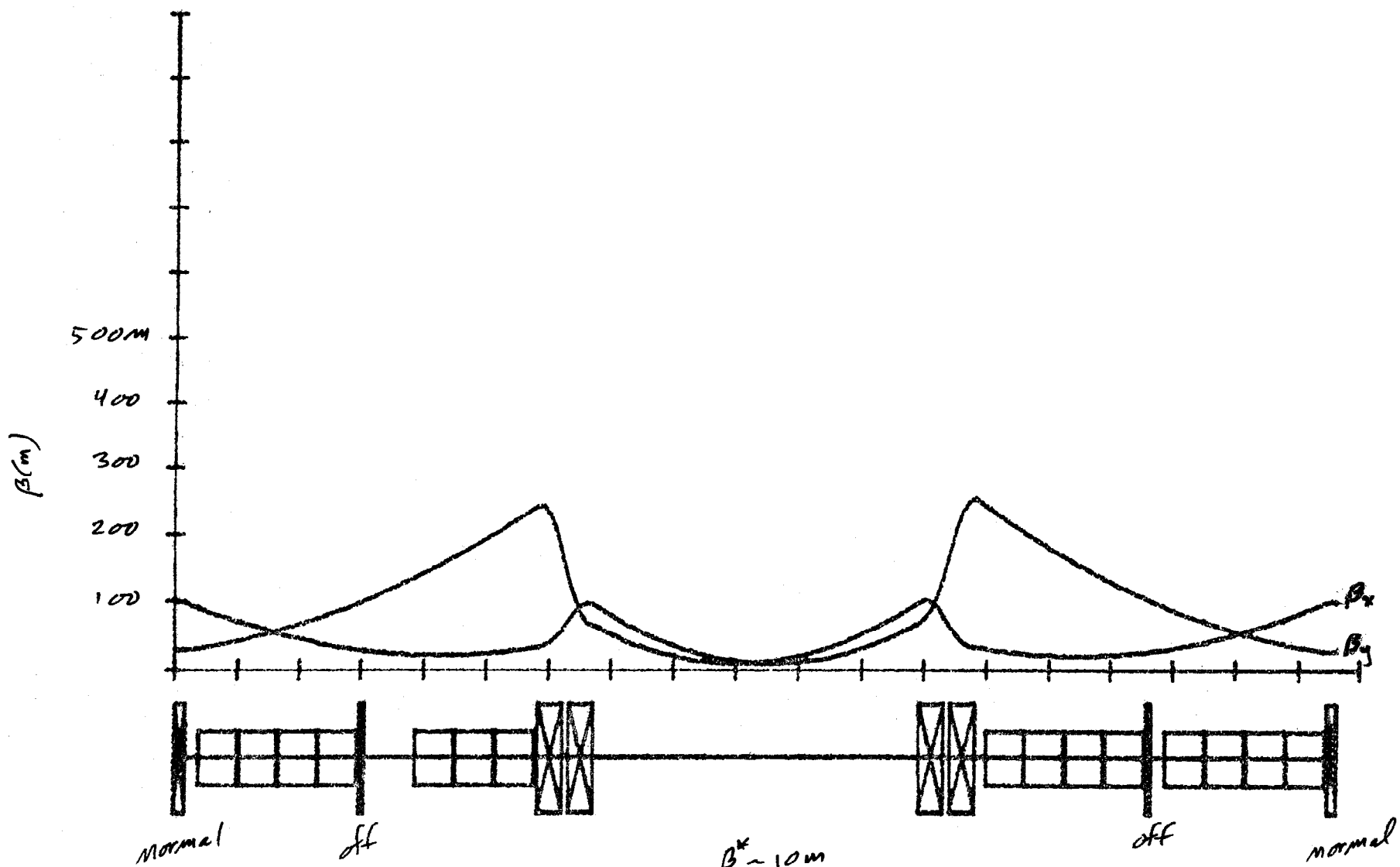
Figure 1



$$\beta^* \approx 77 \text{ m}$$

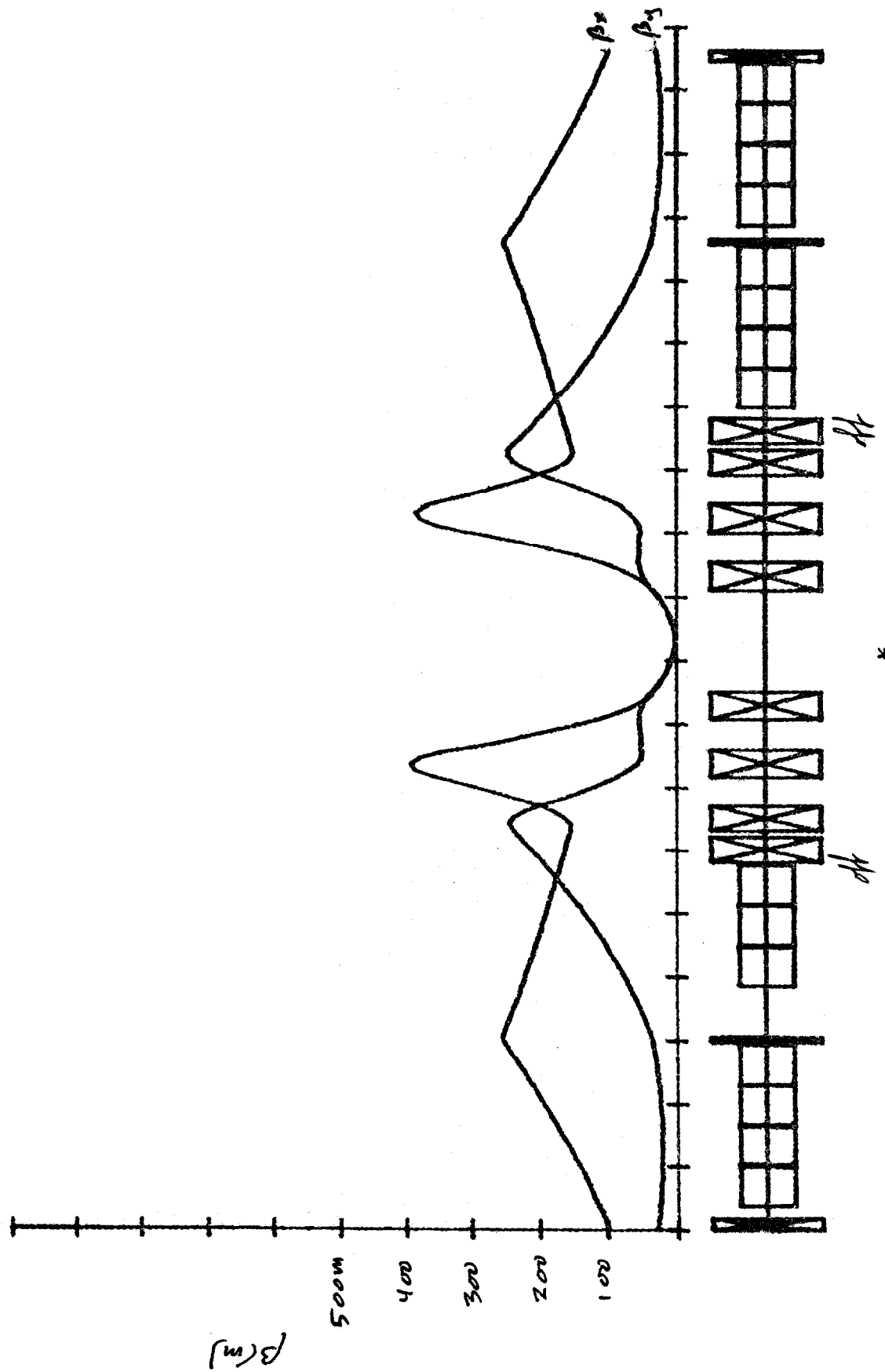
Case A

Figure 2

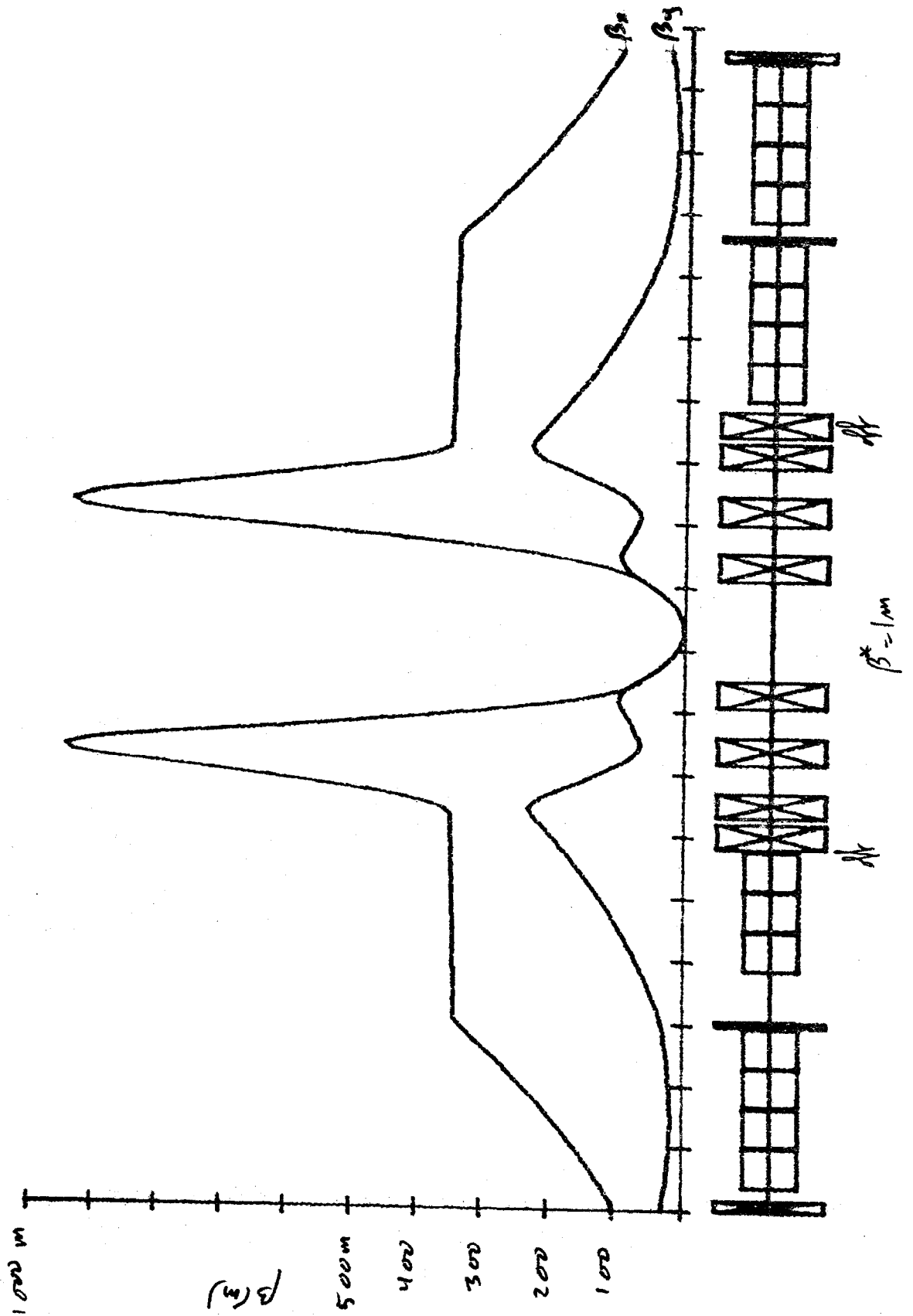


Case B

Figure 3



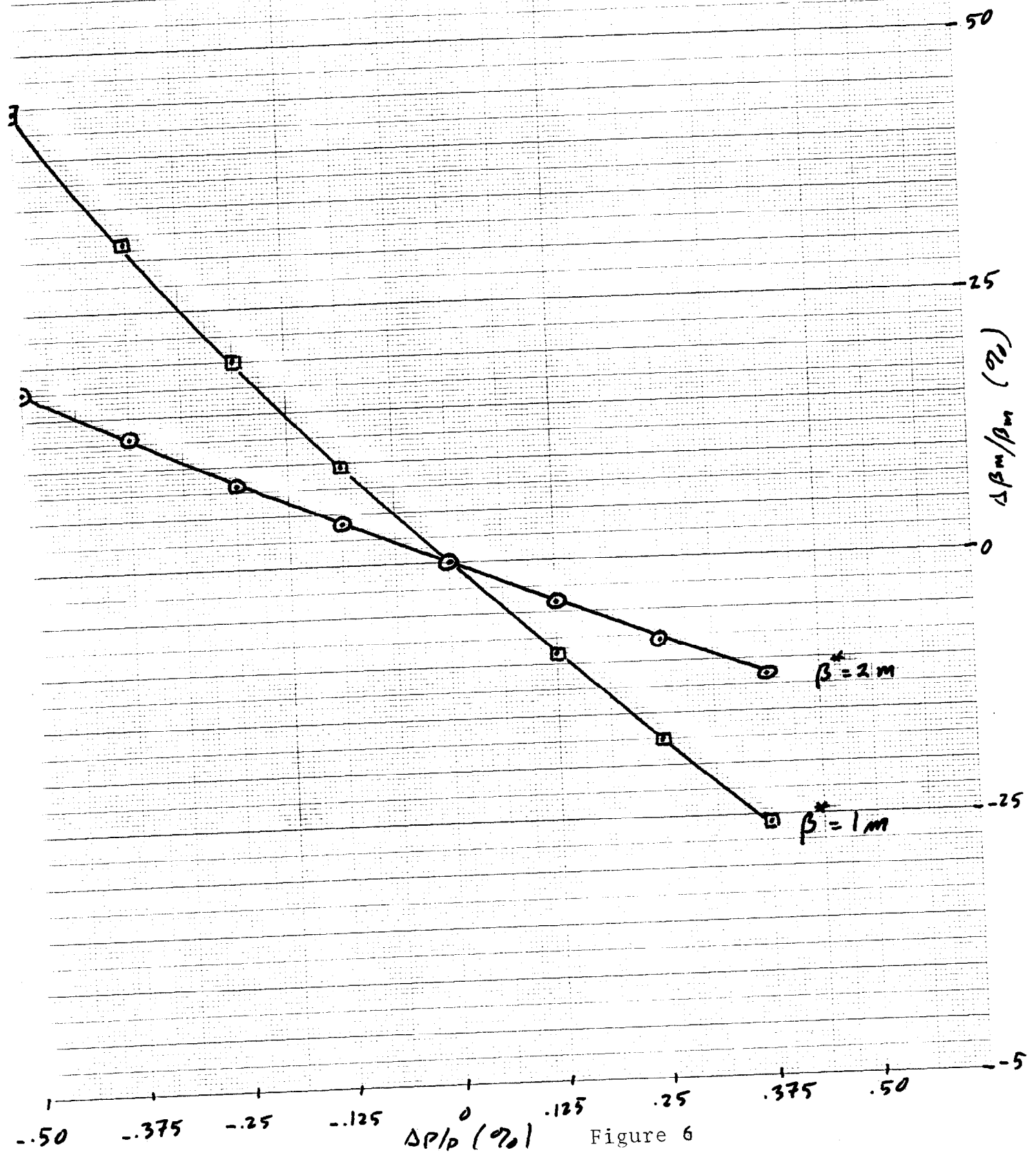
Case C Figure 4

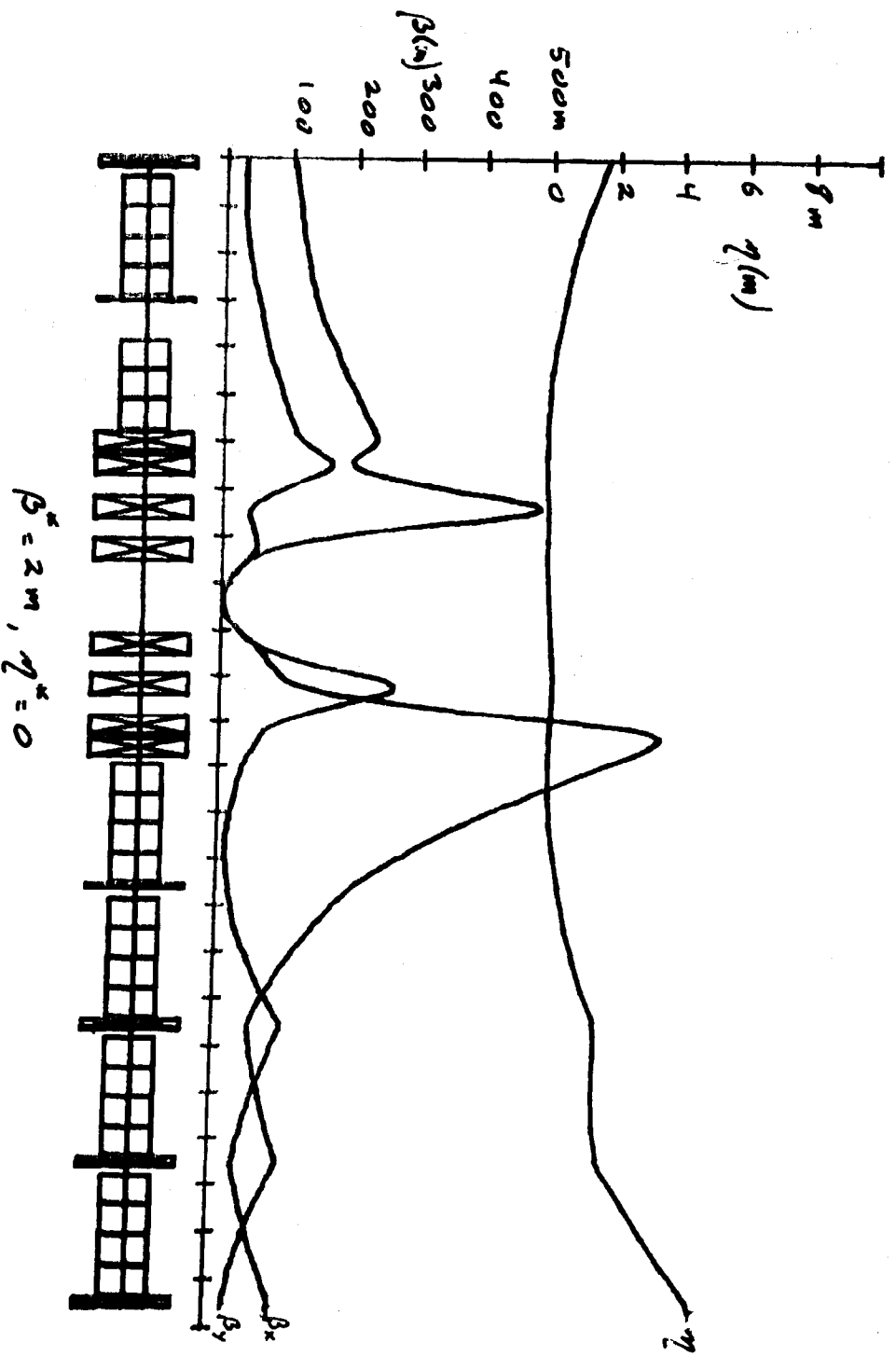


Case D Figure 5

$\Delta \beta_{max} / \beta_{max}$ vs. $\Delta P / P$

TM-876
1700
page 12





Case E

Figure 7